Received: 3 October 2023 | Revised: 30 November 2023 | Accepted: 3 December 2023

DOI: 10.1002/mp.16897

RESEARCH ARTICLE

MEDICAL PHYSICS

Range shifter contribution to neutron exposure of patients undergoing proton pencil beam scanning

Maite Romero-Expósito[1,2] | **Malgorzata Liszka**[1] | **Athanasia Christou**[1] | **Iuliana Toma-Dasu**[2,3] | **Alexandru Dasu**[1,4]

[1]The Skandion Clinic, Uppsala, Sweden

[2]Oncology Pathology Department, Karolinska Institutet, Solna, Sweden

[3]Medical Radiation Physics, Stockholm University, Stockholm, Sweden

[4]Medical Radiation Sciences, Department of Immunology, Genetics and Pathology, Uppsala University, Uppsala, Sweden

Correspondence
Maite Romero-Expósito, Cancercentrum Karolinska, Karolinska Sjukhuset i Solna Visionsgatan 56A, våning 3, 171 76 Stockholm, Sweden.
Email: maite.romero@skandion.se

Funding information
Euratom's research and innovation programme 2019–2020, Grant/Award Number: 945196

Abstract

Background: Superficial targets require the use of the lowest energies within the available energy range in proton pencil-beam scanning (PBS) technique. However, the lower efficiency of the energy selection system at these energies and the requirement of a greater number of layers may represent disadvantages for this approach. The alternative is to use a range shifter (RS) at nozzle exit. However, one of the concerns of using this beamline element is that it becomes an additional source of neutrons that could irradiate organs situated far from the target.

Purpose: The purpose of this study is to assess the increase in neutron dose due to the RS in proton PBS technique. Additionally, an analytical model for the neutron production is tested.

Methods: Two clinical plans, designed to achieve identical target coverage, were created for an anthropomorphic phantom. These plans consisted of a lateral field delivering an absorbed dose of 60 Gy (RBE) to the target. One of the plans employed the RS. The MCNP code was used to simulate the plans, evaluating the distribution of neutron dose equivalent (H_n) and the equivalent dose in organ. In the plan with the RS plan, neutron production from both the patient and the RS were assessed separately. H_n values were also fitted versus the distance to field edge using a Gaussian function.

Results: H_n per prescription dose, in the plan using the RS, ranged between 1.4 and 3.7 mSv/Gy at the field edge, whereas doses at 40 cm from the edge ranged from 9.9 to 32 μSv/Gy. These values are 1.2 to 10 times higher compared to those obtained without the RS. Both this factor and the contribution of neutrons originating from the RS increases with the distance from field edge. A triple-Gaussian function was able to reproduce the equivalent dose in organs within a factor of 2, although underestimating the values.

Conclusions: The dose deposited in the patient by the neutrons originating from the RS predominantly affects areas away from the target (beyond approximately 25 cm from field edge), resulting in a neutron dose equivalent of the order of mSv. This indicates an overall low neutron contribution from the use of RS in PBS.

KEYWORDS
analytical modelling, neutron dose equivalent, out-of-field dose, proton therapy

1 | INTRODUCTION

The use of proton pencil beam scanning (PBS) has seen a rapid growth in recent years, replacing passive scattering as the proton delivery technique in new facilities. Its potential for sparing normal tissues resides in the interaction properties of protons resulting in dose deposition curves with a Bragg peak at the end of the range. While this feature is intrinsically advantageous for deep seated targets, superficial targets require the use of the lowest energies within the available energy range. For example, achieving a depth of 2 cm in water would require an energy of approximately 47 MeV. However, current PBS systems present limitations in their minimum deliverable energy.[1] The energy selection system in fixed-energy production systems, such as cyclotrons, exhibits a gradual reduction in efficiency as energy decreases.[2] For instance, the IBA system (Ion Beam Applications, Louvain-La-Neuve, Belgium) offers an efficiency of the beam after the energy selection system and beam transportation lower than 1.5% for proton energies lower than 100 MeV.[3] Moreover, at low energies, the proton beams exhibit less range straggling, and hence the Bragg peaks width decreases.[4] As a result, more energy layers are required at shallower depths compared to those deeper located to cover a given target thickness.[2,4] In turn, more energy layers lead to longer treatment times, also increasing the probability of intra-fractional movement and patient discomfort.

It is therefore quite common for the treatment of superficial targets to use a range shifter (RS), which is a slab of material inserted into the beam path that acts as a pre-absorber degrading the proton range in tissue and accommodating a reasonably high initial beam energy,[4] and also reducing the needed number of energy layers to cover the target. Unfortunately, this advantage comes at the cost of increasing the spot size and, consequently, decreasing the dose conformality.[3] This can be mitigated by reducing the distance between the RS and the patient surface, thus allowing a smaller possible spot size at entrance. A small air gap also results in a better calculation accuracy of the treatment planning system (TPS).[5]

Nevertheless, the RS becomes an additional external source of neutrons during the proton treatment, increasing the out-of-field doses in proton patients, especially when taking into account the high radiobiological effectiveness of neutrons. Even though in PBS the out-of-field neutron dose is relatively small,[6] measurements in air and inside an anthropomorphic phantom during irradiations with a RS showed that this element could increase the production of neutrons by a factor of around 2 or 3,[7,8,9] while the overall neutron production in PBS is lower than in passive scattering delivery. Therefore, the evaluation of the contribution of RS neutrons in the patient is warranted.

The position of the RS also plays a role in neutron production. As discussed before, in terms of spot size, it is preferable to choose a position as close as possible to the patient. However, studies in passive scatter facilities have showed the decrease of organ doses by increasing the air gap.[10] A similar behavior is expected in the case of the RS and, therefore, an optimal configuration in terms of proton dose distribution within the target is unfavorable in terms of neutron production and thus unwanted dose deposition in organs at risk. Therefore, the aim of this study was to investigate the impact of RS by comparing the distribution of neutron dose equivalent inside a patient when the RS is used for a relatively shallow brain target. This was achieved through the use of Monte Carlo (MC) simulations which allow to separate the contribution of neutrons coming from the RS from the other dose depositions. General purpose MC simulation is considered the gold standard for evaluating stray doses, but it is impractical for routine use in the clinic due to the simulation time. Therefore, an additional aim of our study was to test a simpler empirical analytical model for fast calculations.

2 | METHODS

2.1 | Treatment plans

Two clinical plans for proton PBS were created with the clinical beam model at the Skandion Clinic (Uppsala, Sweden) to treat a superficial target (3 cm depth, 131 cm^3 PTV volume) located on the right side of the brain of an anthropomorphic adult phantom (PBU-60, Kyoto Kagaku, Kyoto, Japan). A CT scan of the phantom was acquired and imported into the Eclipse TPS (Varian Medical Systems, Palo Alto, USA) following the clinical workflow. Each plan used one lateral proton beam delivering 30 fractions of 1.82 Gy per fraction to the target volume to a total of 60 Gy (RBE) assuming an $RBE_{proton} = 1.1$. The first plan, referred to as the plan without RS (NRS plan), consisted of 21 energy layers, ranging from 60 to 97 MeV. The second plan, with the RS, consisted of 14 layers, from 93 to 124 MeV. The RS used in thus study was made of Lexan with a water equivalent thickness of 3.5 cm. The RS was placed as close as possible to the patient, at 25.4 cm from isocenter (located within the target). This setup allowed us to assess the worst-case scenario in terms of neutron exposure of the patient.

2.2 | Monte Carlo simulations

The Monte Carlo N-Particle (MCNP) code, version 6.2[11], was used to assess the neutron production. The primary proton beam MC model was benchmarked

against the Integral Depth Dose (IDD) curves and spot sizes measured during commissioning at the Skandion Clinic (Uppsala, Sweden).[12] Additionally, spot sizes measured during irradiations using RS were used to fine-tune the model.

To simulate the treatment plans, in-house Octave (GNU Octave version 6.4.0) scripts were created to transform the phantom CT and the RTPLAN (both in DICOM format) into the MCNP input format. The resolution of CT image (512×512×211) was reduced to 128×128×211 with a voxel size of 3.9×3.9×5 mm^3 to ensure reasonable simulation times. Each voxel´s density and material were defined according to a stoichiometric calibration.[13] Separate input files were generated for each energy layer in the plan, each containing the actual spatial distribution of the spots.

Neutron dose equivalent (H_n) in each voxel was calculated using a method[14] involving the convolution of the neutron energy spectra, and the kerma (k)[15] and radiation quality (Q) factors.[16] This calculation was implemented with a *F4 tally* together with the *Dose Energy* (DE) and *Dose Function* (DE) cards.[11] To calculate the equivalent dose in organ from voxel values, the delineated structures (from RSTRUCTURE DICOM file) were used to identify the voxels representing each organ and then, averaging the dose equivalent over all of them.

For the study of the RS plan, simulations of the entire irradiation were performed, similar to the NRS plan. However, in addition, the contribution of the patient and the RS were assessed separately. To achieve this, two phase spaces were created scoring the protons after crossing the RS and the neutrons produced in the RS using a *Surface Source Write* (SSW) card.[11] Then, each type of particle was simulated impinging on the phantom in two different runs with the appropriate options specified in a *Surface Source Read* (SSR).[11]

All simulations were conducted with a total source proton number ranging between 1 and 3×10^9 to ensure a suitable statistical uncertainty. However, proton dose validation with measurements (see next section) and comparison with TPS calculation were used as a more accurate estimation of the uncertainty in the MC model. In the case of neutrons, the uncertainty in neutron dose equivalent is mainly influenced by the calculation process based on the kerma approximation and the physics models used in the MC code.[17] Considering these facts, the uncertainty in the neutron contribution was estimated at approximately 20%, which is in line with similar neutron dose determinations.

2.3 | Validation of simulations

As the physical phantom for which the treatments were planned does not have inserts for detectors, it was not possible to validate the neutron production through direct measurements within it. Therefore, a simpler approach was employed for model validation with irradiations performed on a slab phantom for both measurement and simulation purposes. The setup involved irradiating a solid water phantom ($30 \times 30 \times 14$ cm^3) with monoenergetic proton beams, with a field size of 10×10 cm^2. These irradiations were carried out at three different energies, with and without the RS (see values in Table S1). Inside the phantom, a Roos ionization chamber (Type 34001, PTW Freiburg GmbH) was positioned at a depth of 2 cm (at the plateau region of the Bragg Peak), at the isocenter of the proton field, to determine the proton absorbed dose with an uncertainty of 2%. Additionally, at a distance of 120 cm from the phantom, on the treatment couch, a LB 6411 ambient neutron monitor[18] was placed to determine the neutron ambient dose equivalent (H*(10)). The sensitive volume of the neutron monitor was set at the same height as the treatment isocenter. The measurements conducted using the LB 6411 monitor have a 10% uncertainty in neutron fields with energies up to 20 MeV. However, when exposed to higher energies, to which the neutron monitor is not sensitive, underestimations exceeding 50% have been observed.[19] To minimize the influence of high-energy neutrons, the monitor's position was chosen at an angle of 90 degrees from the primary beam direction. This positioning was shown to reduce the contribution of high-energy neutrons to the measurements,[19,20] being the underestimation of the order of 25%.[19]

The simulation of the irradiation conditions incorporates the walls of the facility to account for the neutron scatter in the room, which is relevant for the response of the LB neutron monitor. Proton absorbed dose in the sensitive volume of the Roos chamber (0.35 cc) and neutron spectra at the position of the sensitive volume of the neutron monitor were scored. To calculate H*(10), the neutron spectrum was convoluted with neutron monitor response[18] and the fluence to H*(10) conversion coefficients from ICRP 74.[21]

Finally, the proton dose distributions from the brain plans were compared to the distributions obtained by the TPS to validate the accuracy of the modelling. A 3D gamma function was evaluated within the region enclosed by the 5% isodose line, using a criterion of 5%/7.8 mm. The spatial criterion was determined by the voxel size of the MC phantom used in the simulations and therefore suitable for the simulated geometry.

2.4 | Modelling neutron dose equivalent per absorbed dose (Hn/D)

The analytical model for internal neutrons developed by Gallagher and Taddei[22] was tested with the H_n/D distributions obtained from simulations. This model relies on a double-Gaussian function with a total of 6 parameters, where a different set of parameters is used for protons beams with an energy ≤ 160 MeV and with

an energy > 160 MeV. The mathematical function is represented as follows:

$$\frac{H_n}{D} = \frac{\alpha_1}{\sqrt{2\pi\sigma_1^2}} e^{-\frac{(r-\mu_1)^2}{2\pi\sigma_1^2}} + \frac{\alpha_2}{\sqrt{2\pi\sigma_2^2}} e^{-\frac{(r-\mu_2)^2}{2\pi\sigma_2^2}} \quad (1)$$

where α_i, σ_i and μ_i are the fitting parameters and r, the minimum distance of the voxel to the field edge (defined as the 50% isodose surface inside the phantom). The model was trained for the internal neutrons produced during the intracranial irradiation of a 9-year-old girl, using three proton beams, and tested against two intracranial fields of a 10-year-old boy. The model is purely empirical, not attempting to describe any physical phenomenon and, therefore, although it was designed for internal neutrons, its performance was also tested with the data of the RS plan.

For model testing, the average H_n/D value over all voxels at the same distance from the field edge was calculated. This averaged value was then fitted versus the distance using the model in Equation (1). After fitting, the obtained function was used to calculate the H_n/D in each voxel of the phantom. Subsequently, the equivalent dose in organ was computed, as explained in Section 2.2.

3 | RESULTS

3.1 | Validation of MC model

The differences between experimental and calculated absorbed doses are on average within 3%. However, when it comes to the neutron quantity, the differences are higher. H*(10) is notably dependent on the level of detail used when modelling the treatment room. For this study, only concrete walls were considered, although other materials may also be present in reality. Despite this, the differences between the measured and simulated values are still below 20%. This is considered a satisfactory result as in a comprehensive study focused on the simulation of H*(10) in proton therapy facilities, differences up to 50% were obtained.[7] (See Table S1 for the comparison of measured and calculated values of proton absorbed dose and H*(10) during the validation irradiations.)

3.2 | Brain plans

Figure 1 illustrates the proton dose distribution of the NRS and RS plans obtained by the TPS and the MC simulation. The MC simulation reproduced the relative distribution of the dose in the target area. Seventy percent of the voxels passed the 3D gamma criterion for both plans. The majority of voxels failing the criterion were located in the gradient area around the target. Regarding the absolute dose values, the TPS mean dose in the CTV was 54.6 Gy, whereas the MC simulation yielded a mean dose of 53.1 Gy for the NRS plan. With the use of the RS, the TPS and MC mean doses in the CTV were 54.2 and 51.3 Gy, respectively. Therefore, the results demonstrate a difference of 3%–5% compared to the TPS, indicating good agreement and suitable for the subsequent analysis of the neutron production.

3.3 | Neutron distributions

The distribution of H_n inside the phantom is depicted in Figure 2 for both the NRS and RS plans at the depth of isocenter. Higher values were observed around the target area, and as the distance from this area increases, H_n exhibited a fast decrease (note that plots are on a logarithmic scale). As expected, the RS plan led to higher doses, which is particularly noticeable in the thorax and abdomen regions of the phantom, with a 4–6 increment factor, as shown in Figure 3.

Figure 4 depicts the maximum, minimum and mean values of H_n/D as a function of distance. For the NRS plan, H_n/D at the field edge ranged from 1.2 to 3.3 mSv/Gy. Farther, at approximately 40 cm from field edge, doses were in the μSv/Gy range, in particular, between 1.1 and 7.3 μSv/Gy. For the RS plan, the H_n/D intervals were between 1.4 and 3.7 mSv/Gy at the field edge, while at 40 cm from the edge, dose were in the range of 9.9 to 32 μSv/Gy. The variation in H_n/D at a fixed distance was influenced by the relative position regarding the beam direction. In general, voxels situated behind the target, in the forward direction of the proton beam, received higher doses (see Figure S1). This observation is attributed to the contribution of high-energy neutrons, which are mainly forward directed and less significant in lateral positions. As a result, not only the doses were higher, but the decrease with distance was less pronounced (as illustrated by Figure S1 in the supplementary material). This explains the abrupt drop in the maximum value at approximately 10 cm in both plots in Figure 4. Since the target is located in the head region, the size of the body behind the target is thinner than 10 cm from field edge. Consequently, at greater distances, there was no contribution of voxels in the forward direction. This also influenced the shape of the mean H_n/D curve. In contrast, the minimum H_n/D curve, primarily defined by lateral voxels, exhibits a smoother dependence.

For the RS plan, the contributions to H_n from neutrons produced in the RS and those produced by the proton beam impinging on the phantom were evaluated separately (see Figure S2). The results indicated a small contribution to the dose from the neutrons originating in the RS in the head, accounting to below 20%. The contributions increased to about 40% to 60% in the upper

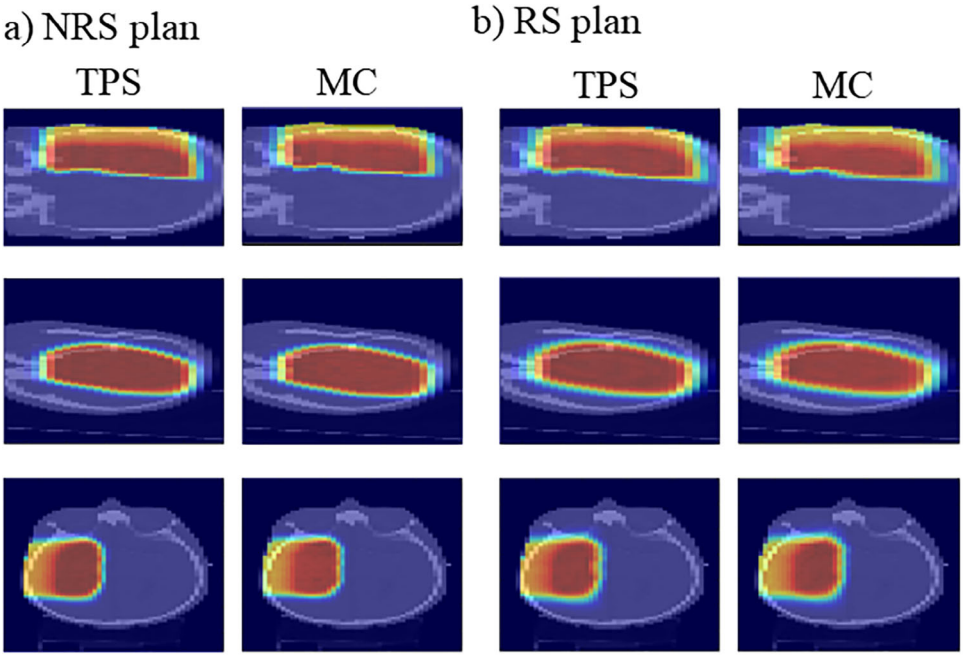

FIGURE 1 Proton absorbed dose distribution for the NRS (a) and RS (b) plans. Distribution obtained by TPS on the left and by MC on the right. Coronal, sagittal, and axial views at the depth of isocenter from top to bottom. TPS, treatment planning system; MC, Monte Carlo; RS, range shifter.

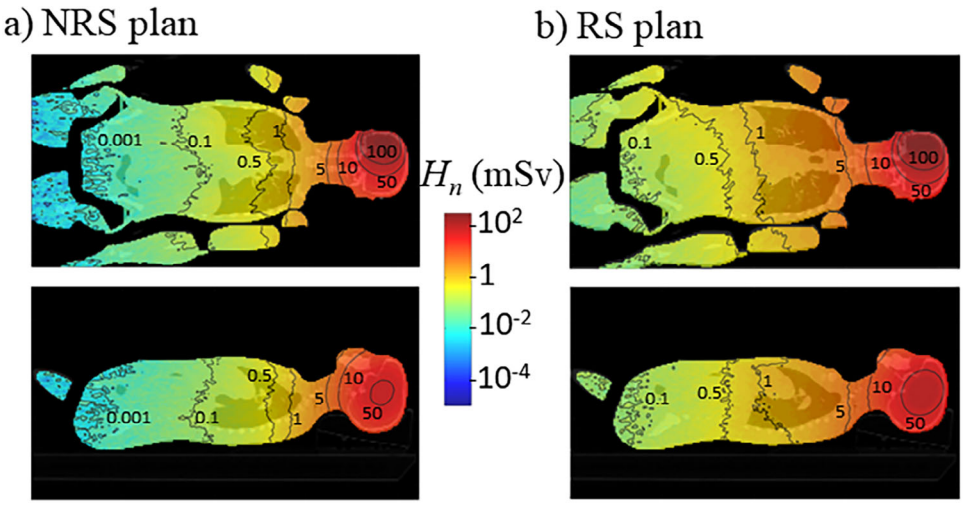

FIGURE 2 Neutron dose equivalent distribution inside the phantom for the NRS (a) and RS (b) plans. Contour lines for some dose values were included for guidance. Coronal and sagittal view at the depth of isocenter, from top to bottom. Notice that plots are in logarithmic scale. RS, range shifter.

part of the thorax, while neutrons from RS became predominant in the rest of the body. This variation in the relevance of the RS was also evident in Figure 4 when comparing the rate of reduction of the values. Up to approximately 10 cm, the behavior was similar, but beyond, the values decreased faster for the NRS plan.

In terms of the neutron equivalent dose in organ, surrounding organs to target inside the head received doses around 2 mSv/Gy with the RS and 1.5 mSv/Gy without it (see Table 1). This order of magnitude reduced to tens of μSv/Gy when moving to the thorax and beyond. For example, in lungs without the RS, neutron equivalent dose was, on average, 9.5 μSv/Gy. As demonstrated earlier, the increase in dose due to the RS was more significant in this area than in the head, reaching a mean value of 36 μSv/Gy. In the liver, equivalent dose increased from 2.5 to 14 μSv/Gy due to the use of the RS. Table 1 also highlights that the dose attributable to the RS ranges from 5 to 83 μSv/Gy.

TABLE 1 Equivalent dose in organ per absorbed dose (in μSv/Gy) due to neutrons in NRS and RS plans.

		RS plan			
Organ	NRS plan	Total	Neutrons from patient	Neutrons from RS	RS/NRS
Brain	1.4×10^3	1.9×10^3	1.9×10^3	69	1.4
Brain stem	1.6×10^3	2.2×10^3	2.1×10^3	69	1.4
Chiasm	1.5×10^3	2.1×10^3	2.0×10^3	71	1.4
Right eye	6.5×10^2	1.0×10^3	9.4×10^2	83	1.6
Left eye	4.0×10^2	6.1×10^2	5.5×10^2	53	1.5
Spinal channel	38	82	54	26	2.1
Right lung	9.9	40	13	27	4.1
Left lung	8.9	32	12	19	3.5
Heart	3.7	25	4.6	20	6.8
Spleen	2.3	12	3.4	8.7	5.0
Liver	2.5	14	3.5	10	5.4
Right kidney	1.5	7.4	1.8	5.2	5.0
Left kidney	1.2	7.2	1.5	5.7	6.1

Abbreviation: RS, range shifter.

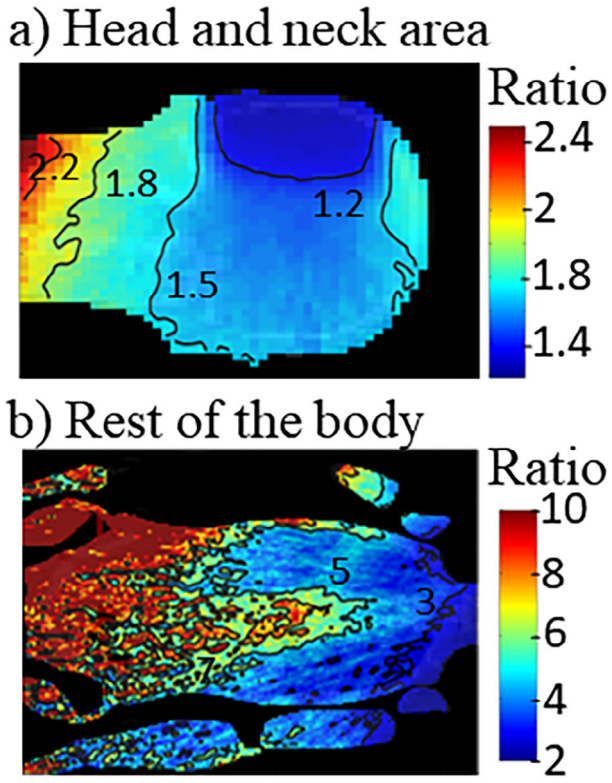

FIGURE 3 Ratio between neutron dose equivalent (H_n) in the RS and NRS plan for the head and neck area (a) and the rest of the body (b). Notice the change of scale between plots. RS, range shifter.

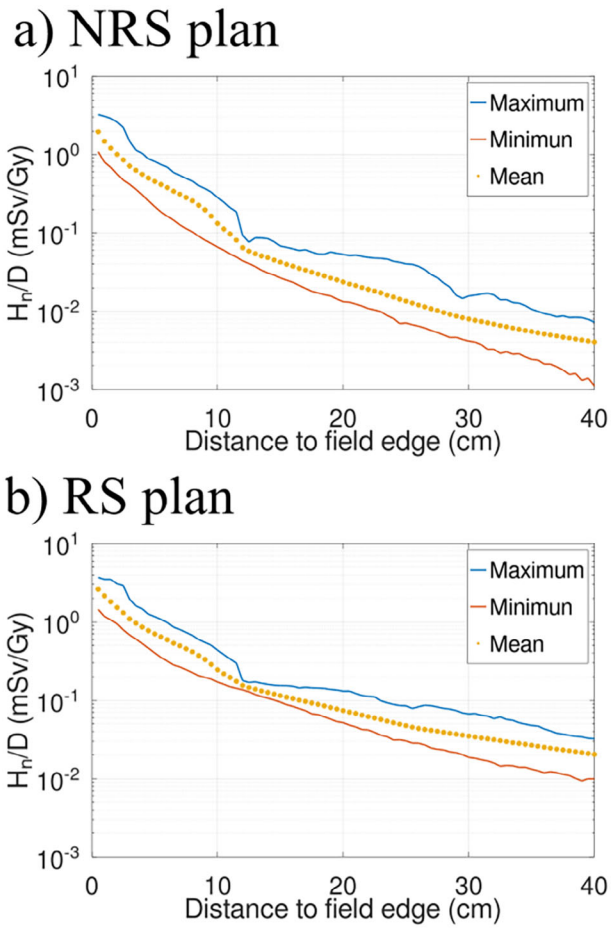

FIGURE 4 Neutron dose equivalent per absorbed dose (H_n/D) versus distance to field edge for the no range shifter (NRS) (a) and RS (b) plans. For each distance, maximum, minimum, and mean values are plotted. RS, range shifter.

3.4 | Analytical model testing

The results of the simulations were also fitted with the empirical double-Gaussian function, as depicted in Figure 5 for both plans. The coefficient of determination

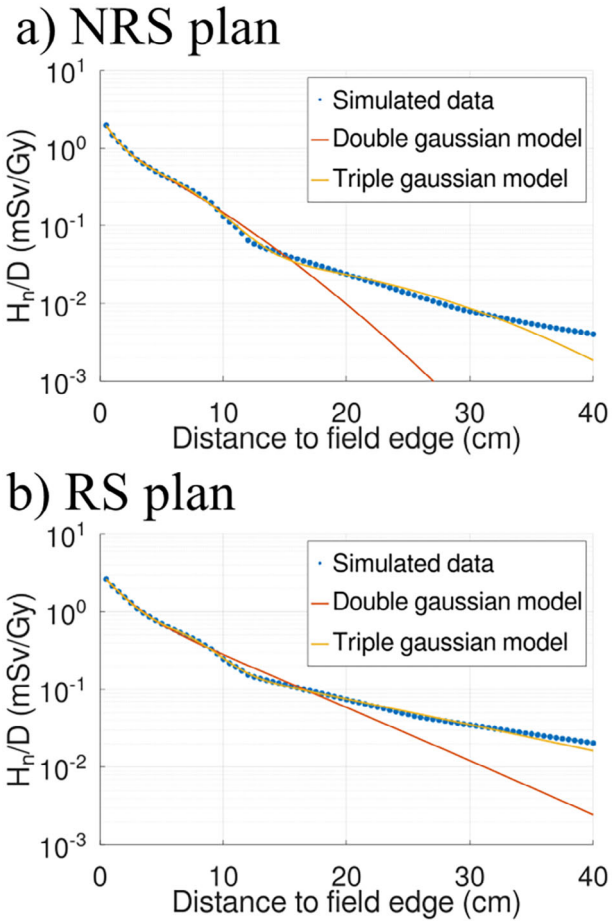

FIGURE 5 Mean neutron dose equivalent per absorbed dose (H_n/D) versus distance to field edge for the NRS (a) and RS (b) plans. Analytical models based on mathematical model from Gallagher and Taddei[22] using double- and triple-Gaussian functions are also represented. RS, range shifter.

($r2$) obtained was 0.998 and 0.997 for the NRS and RS plan, respectively, indicating that the analytical mathematical function would work reasonably well. However, as seen in the figure, the model diverged from the data starting from approximately 15 cm onwards, indicating that the mathematical function is not fully able to reproduce the entire behavior accurately. This was however not reflected in the coefficients of determination because of the small values of the doses, as highlighted by the use of a logarithmic scale in the plot. Differences between the simulated and estimated values were, in general, below approximately 20 μSv/Gy (as shown in Figure S3) or a total of 1 mSv for the total prescription of the plan. In addition, the main drawback is that the model tends to underestimate the dose. In order to improve the predictions of the analytical model, we have also tried to introduce a third Gaussian component into the expression in Equation (1). This has resulted in a general improvement of the fit (with r^2 equal to 0.9996 and 0.99991, respectively) as illustrated in Figures 5 and S3. Nevertheless, at a few centimeters from the field edge, the underestimation could reach up to 40 μSv/Gy in the case of the NRS plan. For the RS plan, differences between the model and the simulated doses were below 20 μSv/Gy.

TABLE 2 Ratio between MC and estimated equivalent doses in organ using the double- and triple-Gaussian model.

	NRS plan		RS plan	
Organ	**Double**	**Triple**	**Double**	**Triple**
Brain	1.4	1.4	1.3	1.3
Brain stem	1.3	1.3	1.2	1.2
Chiasm	1.3	1.3	1.2	1.2
Right eye	0.93	0.95	1.0	1.0
Left eye	1.1	1.1	1.1	1.1
Spinal channel	0.78	0.74	0.89	0.82
Right lung	6.7	1.1	2.5	1.1
Left lung	8.1	1.1	2.2	0.93
Heart	[a]	1.1	5.7	1.2
Spleen	[a]	5.4	[a]	1.3
Liver	[a]	4.2	[a]	1.3
Right kidney	[a]	[a]	[a]	1.3
Left kidney	[a]	9.4	[a]	1.2

Abbreviations: MC. Monte Carlo; RS, range shifter.
[a]Values higher than 10.

To assess the practical usefulness of the model, we evaluated the equivalent doses in organs using both the double- and triple-Gaussian models. The ratio between the simulated values and the estimated ones are presented in Table 2. For most of the organs the triple-Gaussian model resulted in a factor lower than 2 between simulated and estimated values, which is a clear improved performance in comparison to the double-Gaussian model. However, both models still tended to underestimate the dose to organs far from the target.

4 | DISCUSSION

Previous studies on the increased neutron exposure from the use of a RS have demonstrated a two- or three-fold increase in doses compared to similar irradiations without the RS.[7,8] However, it is important to note that these studies were based on measurements of H*(10) in the treatment room, and this scenario may not be representative for what happens inside the patient.

To our knowledge, ours is the first study investigating systematically the RS contribution to neutron exposure of patients undergoing proton therapy with PBS. The study was based on the MC modeling of clinical proton beams and the subsequent stray neutron fields, and the voxel-based neutron dose equivalent distribution has been assessed respectively for the same case with and without a RS.

In general, our results are in agreement with an 2-fold increase in neutron dose in areas close to the target (head and neck), at distances up to 12 cm from field edge. However, we observed that in these areas, the contribution to dose from the neutrons originating on the RS represents only a fraction of the stray dose. In a recent study by Wochnik *et al*.,[9] measurements conducted inside a phantom showed that RS could increase the neutron dose by a factor between 1.5 and 2.2. In this case, measurements were performed in a 5-year-old phantom at distances ranging from 13 to 30 cm from the isocenter. Compared to our simulations, positions located at 30 cm from isocenter are in the upper part of thorax, approximately at the height of the shoulder, where our results indicate a neutron dose increase by an average factor of approximately 3.8. However, when considering the differences in the irradiation conditions between the studies, including the phantom used (manufacturer and age), target size (113 cm^3), proton energy range (from 80 to 140 MeV), RS thickness (4.2 cm water equivalent thickness), and air gap (46 cm from the isocenter), we can conclude that our results are compatible.

In addition, our study analyses farther regions from the target, showing that the effect of RS could be even higher (Figure 4). However, it is worth paying attention to the absolute values of the dose equivalent or equivalent doses in organs. In the area around the target, the use of RS resulted in a maximum dose of approximately 4 mSv/Gy. Taking into account the physical dose prescription for the brain plan (54.6 Gy), this would represent a maximum equivalent dose increase of 218 mSv. In terms of equivalent dose in organ, the most affected tissue, the brain stem, would receive a dose of 120 mSv. However, a crucial point to consider is that in this area, organs are also exposed to the proton field. For instance, the brain stem received a mean dose of 2.0 and 3.6 Gy (RBE) in the NRS and RS plans, respectively, making the contribution of neutrons practically negligible. Similarly, the right eye was exposed to protons, receiving a mean dose of 505 mGy (RBE) in the RS plan in comparison to only 56 mSv due to neutrons. It is important to remark that the neutron dose for these closer organs to the target is mainly attributed to the secondary neutrons produced by the proton beam, which is an unavoidable source of neutrons regardless of whether the beam uses an RS or not. Therefore, the RS could be regarded as having a modulating effect, mainly altering the distribution of protons and to a second extent increasing the neutron doses to the patient. An explanation to this behavior resides in the interaction processes leading to the generation of neutrons. The proton beam scored after the RS presented a component of higher energies in comparison to the NRS plan. Since the neutron production increases with proton energy,[10] these more energetic protons in the RS plan explain why doses due to the neutrons originated in the phantom are generally higher than in the NRS plan (as illustrated by the values of equivalent doses in organ in Table 1). Nevertheless, the more energetic protons are producing more high energy neutrons which are forward directed and not likely to contribute to doses to distant organs and tissues. On the other hand, in regions where the main neutron dose contribution comes from the RS neutrons, such as the lungs, the total equivalent dose is considerably lower, approximately 2.2 mSv for the whole plan. In simple terms, where the direct effect of RS is more relevant, doses are relatively low, of the order of mSv, and therefore the contribution to the total integral dose is low.

In our study, we have also tested the performance of the analytical model from Gallagher and Taddei[22] to predict out-of-field neutron doses. While we assumed that the mathematical model would be generally applicable, our results revealed some differences. Thus, the Gallagher and Taddei model found an overestimation of the H_n/D values for distances higher than 10 cm, while our fitted functions tended to underestimate the dose, even after adding the third Gaussian to the model. The overestimation of the Gallagher and Taddei model explains the better performance on the RS plan, given that doses are higher. The origin of the underestimation in our work can be attributed to the shape of our data and the shoulder observed around 10 cm. The Gaussian model, especially the double-Gaussian function, presents a shape more similar to the smooth curve of the minimum H_n/D from Figure 4. Given the low level of the absolute doses involved, it becomes challenging to accurately reproduce the observed data with an analytical model. Our estimations with the triple-Gaussian model were in general within a factor of difference below 2, whereas the Gallagher and Taddei model resulted in a factor between 2 and 3, which is acceptable given the uncertainties in simulations and differences in irradiation conditions. In terms of absolute values, the triple-Gaussian model provides a closer approximation to the actual data. Differences on the order of 1 mSv over the course of the treatment could be acceptable, considering the benefits of rapid calculations using a simple model.

When analyzing Figure 4, the variations in H_n/D for positions at the same distance from target were attributed to the different relative position regarding the direction of the proton beam. This phenomenon is a result of the directional production of high-energy neutrons, which significantly contribute to the dose. The use of only one beam to cover the target accentuates this dependence on the angular position. In other words, employing several beam angles could potentially minimize the variations within the same distance. In Gallagher and Taddei,[22] the training data was relevant for plans with three fields: a left and a right posterior oblique field, and a posterior anterior field. Since they presented only averaged H_n/D values, it was not possible to infer

whether their data exhibit similar variations as observed in our results. Our hypothesis is that the use of more beams would result in smoother curves of H_n/D versus distance, reducing the shoulder in the plot, and allowing a better performance of the Gaussian functions, at least reducing the underestimation observed in our current results. Further studies of clinical cases are therefore needed to advance the development of general analytical models, ensuring their applicability and accuracy in clinical settings.

Nevertheless, our results also showed that neutron production in active scanning proton beams in several orders of magnitude lower than in passively scattered beams and that the RS contribution to the integral dose is very low.

5 | CONCLUSIONS

The increase in neutron dose equivalent and equivalent dose in organ due to the use of the RS has been assessed through MC simulation for a brain treatment. On one hand, there is a direct effect caused by the neutrons originating from the RS, which deposit dose in the patient. This effect predominantly affects areas away from the target, resulting in a neutron dose equivalent of the order of mSv (or a few tens of μSv/Gy). On the other hand, there is an indirect effect due to the increase in the energy of the proton beam reaching the patient, which consequently leads to an increase in the neutron production within it. This indirect effect mainly affects the region around the target, resulting in a neutron dose equivalent of up to a few hundreds of mSv (or a few mSv/Gy). However, it is important to note that this region can also be exposed to the proton field, making the neutron component almost negligible in comparison.

The use of a simple analytical model for the estimation of the neutron contamination within the patient was not entirely satisfactory due to a systematic underestimation of the dose.

ACKNOWLEDGMENTS

MRE thanks Dr Ureba and Dr Almhagen for the support in scripting. This project has received funding from Euratom's research and innovation programme 2019–2020 under grant agreement no. 945196.

CONFLICT OF INTEREST STATEMENT

The authors declare no conflicts of interest.

REFERENCES

1. Lin H, Shi C, Huang S, et al. Applications of various range shifters for proton pencil beam scanning radiotherapy. *Radiat Oncol*. 2021;16:146. doi:10.1186/s13014-021-01873-8
2. Matysiak W, Yeung D, Slopsema R, Li Z. Evaluation of the range shifter model for proton pencil-beam scanning for the Eclipse v.11 treatment planning system. *J Appl Clin Med Phys*. 2016;17:391-404. doi:10.1120/jacmp.v17i2.5798
3. Both S, Shen J, Kirk M, et al. Development and clinical implementation of a universal bolus to maintain spot size during delivery of base of skull pencil beam scanning proton therapy. *Int J Rad Oncol Biol Phys*. 2014;90:79-84. doi:10.1016/j.ijrobp.2014.05.005
4. Titt U, Mirkovic D, Sawakuchi G, et al. Adjustment of the lateral and longitudinal size of scanned proton beam spots using a preabsorber to optimize penumbrae and delivery efficiency. *Phys Med Biol*. 2010;55:7097-7106. doi:10.1088/0031-9155/55/23/S10
5. Shirey R, Wu H. Quantifying the effect of air gap, depth, and range shifter thickness on TPS dosimetric accuracy in superficial PBS proton therapy. *J Appl Clin Med Phys*. 2018;19:164-173. doi:10.1002/acm2.12241
6. Schneider U, Hälg RA. Neutron dose and its measurement in proton therapy-current state of Knowledge. *Br J Radiol*. 2020;93:20190412. doi:10.1259/bjr.20190412
7. Van Hoey O, Stolarczyk L, Lillhök J, et al. Simulation and experimental verification of ambient neutron doses in a pencil beam scanning proton therapy room as a function of treatment plan parameters. *Front Oncol*. 2022;12:903537. doi:10.3389/fonc.2022.903537
8. Eliasson L, Lillhök J, Bäck T, Billnert-Maróti R, Dasu A, Liszka M. Range-shifter effects on the stray field in proton therapy measured with the variance–covariance method. *Front Oncol*. 2022;12:882230. doi:10.3389/fonc.2022.882230
9. Wochnik A, Stolarczyk L, Ambrožová I, et al. Out-of-field doses for scanning proton radiotherapy of shallowly located paediatric tumours—a comparison of range shifter and 3D printed compensator. *Phys Med Biol*. 2021;66:035012. doi:10.1088/1361-6560/abcb1f
10. Romero-Expósito M, Toma-Dasu I, Dasu A. Determining out-of-field doses and second cancer risk from proton therapy in young patients—An overview. *Front Oncol*. 2022;12:892078. doi:10.3389/fonc.2022.892078
11. Werner CJ, Armstrong JC, Brown FB, et al. MCNP User's Manual—Code Version 6.2. Los Alamos National Laboratory, report LA-UR-17-29981. 2017.
12. Ardenfors O, Dasu A, Lillhök J, Persson L, Gudowska I. Out-of-field doses from secondary radiation produced in proton therapy and the associated risk of radiation-induced cancer from a brain tumor treatment. *Phys Med*. 2018;53:129-136. doi:10.1016/j.ejmp.2018.08.020
13. Schneider W, Bortfeld T, Schlegel W. Correlation between CT numbers and tissue parameters needed for Monte Carlo simulations of clinical dose distributions. *Phys Med Biol*. 2000;45:459-478. doi:10.1088/0031-9155/45/2/314
14. Romero-Expósito M, Domingo C, Sánchez-Doblado F, Ortega-Gelabert O, Gallego S. Experimental evaluation of neutron dose in radiotherapy patients: which dose? *Med Phys*. 2016;43:360-367. doi:10.1118/1.4938578
15. Chadwick M, Barschall H, Caswell R, et al. A consistent set of neutron kerma coefficients from thermal to 150 Mev for biologically important materials. *Med Phys*. 1999;26:974-991. doi:10.1118/1.598601
16. Siebert BRL, Schuhmacher H. Quality factors, ambient and personal dose equivalent for neutrons based on the new ICRU stopping power data for protons and alpha particles. *Radiat Prot Dosim*. 1995;58:177-183. doi:10.1093/oxfordjournals.rpd.a082612
17. De Saint-Hubert M, Farah J, Klodowska M, et al. The influence of nuclear models and Monte Carlo radiation transport codes on stray neutron dose estimations in proton therapy. *Radiat Meas*. 2022;150:106693. doi:10.1016/j.radmeas.2021.106693
18. Burgkhardt B, Fieg G, Klett A, Plewnia A, Siebert BRL. The neutron fluence and H*(10) response of the new LB 6411

REM counter. *Radiat Prot Dosim*. 1997;70:361-364. doi:10.1093/oxfordjournals.rpd.a031977
19. Farah J, Mares V, Romero-Expósito M, et al. Measurement of stray radiation within a scanning proton therapy facility: EURADOS WG9 intercomparison exercise of active dosimetry systems. *Med Phys*. 2015;42:2572-2584. doi:10.1118/1.4916667
20. Mares V, Romero-Expósito M, Farah J, et al. A comprehensive spectrometry study of a stray neutron radiation field in scanning proton therapy. *Phys Med Biol*. 2016;61:4127-4140. doi:10.1088/0031-9155/61/11/4127
21. ICRP. Conversion coefficients for use in radiological protection against external radiation. ICRP Publication 74. *Ann. ICRP* 1996;26(3-4).
22. Gallagher K, Taddei P. Analytical model to estimate equivalent dose from internal neutrons in proton therapy of children with intracranial tumors. *Radiat Prot Dosim*. 2019;183:460-468. doi:10.1093/rpd/ncy166

SUPPORTING INFORMATION

Additional supporting information can be found online in the Supporting Information section at the end of this article.

How to cite this article: Romero-Expósito M, Liszka M, Christou A, Toma-Dasu I, Dasu A. Range shifter contribution to neutron exposure of patients undergoing proton pencil beam scanning. *Med Phys*. 2023;1-10. https://doi.org/10.1002/mp.16897